ISSN 1870-4069

Tuning Control Law Gains in an Exoskeleton through Swarm Intelligence

Gerardo Adrián De La Rosa-Hernández, Griselda Quiroz-Compeán, Juan Angel Rodríguez-Liñan, Luis Martín Torres-Treviño

Universidad Autónoma de Nuevo León,
Facultad de Ingeniería Mecánica y Eléctrica,
México

gerardo.delarosahe@uanl.edu.mx

Abstract. Exoskeletons are mechatronic devices that can be used in physical rehabilitation programs for people who have suffered neurological injury such as ischemic or hemorrhagic brain accident. This type of injury can cause partial or total loss of mobility, so it becomes necessary to have assistive devices that support people to recover their mobility and return to their daily life. A typical problem in exoskeleton control is the adjustment of control law gains because it is challenging and lacks precision. For this reason, it seeks to know the appropriate values of the gains of a controller that generate the appropriate input torque in the exoskeleton's joints to solve the low-level control problem, managing to obtain the smallest possible error between the input reference path and the current angular position. To know the appropriate parameters, it is assumed that with the use of optimization tools such as evolutionary computing algorithms or collective intelligence the error signal in a multiple-joint structure, such as the exoskeleton, could be minimized. Comparison between heuristic and intelligent methods shows that objective function could be minimized to obtain best gains values, therefore, intelligent method calculates better performance values in terms of angular position error, so considering the calculated gains, the low-level control has been improved to accomplish with trajectory tracking problem.

Keywords: Exoskeleton, mechatronic assistive device, PID intelligent tuning, particle swarm optimization, integral squared error.

1 Introduction

As per the World Health Organization (WHO), more than 15% of people worldwide experiences some form of disability [5]. In the year 2010, in the United States exclusively, approximately 30.6 million individuals faced disability-related challenges with their mobility, such as having trouble in walking, climbing stairs or descending them, assistance of a wheeled chair, zimmer frame, cane or walking sticks [3].

Talking about the European Union in the year of 2011, is mentioned that there are over 11,000 people with walking disabilities [6]. Based on the National Health and Nutrition Survey of 2012, at a nationwide scale, approximately 4.9% of males and 5.8% of females (equivalent to around 2.5 million and 3 million individuals, respectively) were documented to have a disability affecting their mobility or ability to walk [8].

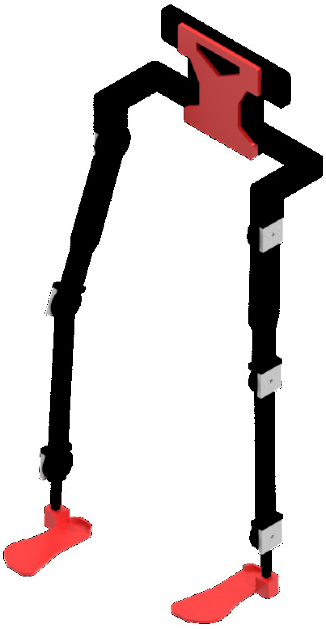

(a)

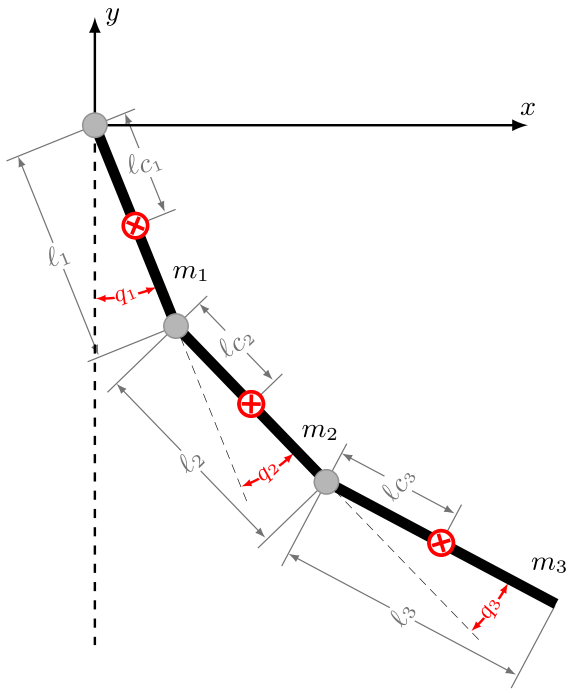

(b)

Fig. 1. (a) Mechanical design of a 6 DOF exoskeleton. (b) Rigid body diagram considered for Euler-Lagrange mathematical modelling.

In the specific case of disabilities in the lower limbs, they may originate from congenital anomalies [24], chronic conditions [4], or injuries [23, 12]. Overall statistics show that disabilities related to neuromuscular pathologies of lower limbs are prevalent. Among these medical conditions is the occurrence of an ischemic or hemorrhagic incident, commonly referred to as a stroke, which occurs when a thrombus obstructs or constricts an artery responsible for supplying blood to the brain.

Some lifestyle related risk factors are being overweight or obese, physically inactive or drinking alcoholic beverages in excess, meanwhile, medical risk factors encompass elevated blood pressure, high cholesterol, diabetes, among other conditions, with one of the prevailing complications being paralysis or impaired muscle movement [14]. To improve the quality of life of a person with such a complication, it is necessary to provide treatment options and therapies so that affected patients can successfully reintegrate into their daily activities.

One tool that may be useful in physical rehabilitation programmes is exoskeletons [19]. The development of mechatronic exoskeletons involves at least the following stages: mechanical design (number of degrees of freedom, kinematic and dynamic capabilities, mechanical constraints), instrumentation (sensor selection, actuators, processing system), control (control modules or algorithms defining the automatic behaviour of the device) [21].

Algorithm 1 PSO pseudocode.

Generate population
for $t = 1$: last generation **do**
    for $i = 1$: population size **do**
        if $f(X_{i,k}(t)) < f(p_i(t))$ **then** $f(p_i(t)) = f(X_{i,k}(t))$
            $f(G_{\text{best}}(t)) = \min(f(p_i(t)))$
        end if
        for $k = 1$ **to** problem dimension **do**
            $V_{i,k}(t+1) = wV_{i,k}(t) + c_1\, r_1(P_{\text{best}} - X_{i,k}(t)) + c_2\, r_2(G_{\text{best}} - X_{i,k}(t))$
            $X_{i,k}(t+1) = X_{i,k}(t) + V_{i,k}(t+1)$
            if $V_{i,k}(t+1) > v_{\max}$ **then** $V_{i,k}(t+1) = v_{\max}$
            else if $V_{i,k}(t+1) < v_{\min}$ **then** $V_{i,k}(t+1) = v_{\min}$
            end if
            if $X_{i,k}(t+1) > x_{\max}$ **then** $X_{i,k}(t+1) = x_{\max}$
            else if $X_{i,k}(t+1) < x_{\min}$ **then** $X_{i,k}(t+1) = x_{\min}$
            end if
        end for
    end for
end for

There is currently a wide variety of exoskeleton concept tests, including some commercial developments, such as the Indego, ReWalk, HAL, Exo-H3 and Ekso GT [19]. Commonly developments include four acting degrees of freedom (hip and knee) [10]. This imposes the challenge of extending the mechanical design to have exoskeletons that consider motion acting on the three main joints of the lower extremities, namely: hip, knee and ankle.

There are direct antecedents on the design and control of exoskeletons as reported in [22] and [2]; however, there are still many questions to be solved in terms of energy modulation of such devices. When discussing exoskeleton control strategies, it is essential to consider the three distinct levels involved: high level, medium level, and low level.

The high-level control pertains to land identification, where the focus lies on identifying and assessing the terrain. The medium-level control is concerned with the operation mode, determining the appropriate mode of operation based on the given circumstances. Lastly, the low-level control aims to achieve the desired torque or position for the articulations involved [1].

This research work develops the dynamic model from the Euler Lagrange equations based in an exoeskeleton model and proposes a PID controller [16] tuned using optimization tools such as swarm intelligence algorithms [20] applied to finding the appropriate gains to solve the low level control problem.

Comparison between two methods shows that objective function could be minimized to obtain best gains values, therefore, intelligent method calculates better performance values in terms of angular position error, so considering the calculated gains, the low-level control has been improved to accomplish with trajectory tracking problem.

Table 1. Dynamic model parameters.

Parameter	Value
Mass (m)	5
Length (ℓ)	0.45
Center of mass length (ℓ_c)	0.01
Inertia moment (I)	0.1595
Viscous friction coefficient (b)	0.17
Coulomb friction coefficient (f_c)	0.45
Gravity (g)	9.8

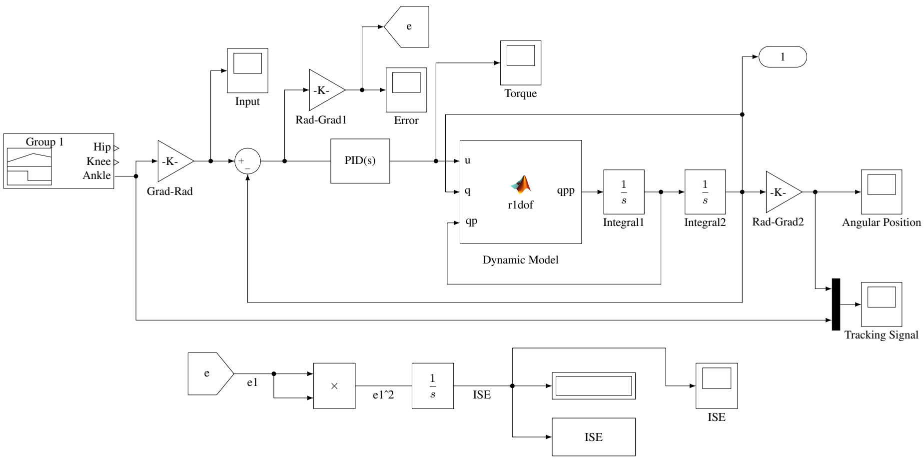

Fig. 2. Diagram developed in MATLAB-Simulink to obtain the trajectory tracking, trajectory error and torque from the three different input signals.

2 Exoeskeleton Mathematical Model

The mechanical design of the exoskeleton seeks to reproduce the joint movement of the lower extremities of the human body as shown in Figure 1a. The resulting mechanism is planar and its movement can be mathematically modeled with the Euler-Lagrange methodology for planar robots.

Because the mechanism reproduces the movement of the lower limb extremities, the model is proposed as a pair of open chains of three degrees of freedom each as shown in Figure 1b. This section describes the methodology for obtaining the dynamic model of one of the open chains, assuming it is the same methodology for two chains.

2.1 Euler-Lagrange Equations

The Euler Lagrange equations describes the dynamics of the articular positions and velocities of a mechanical system and is given by [9]:

$$\tau = \frac{d}{dt}\left[\frac{\partial L(q,\, \dot{q})}{\partial \dot{q}}\right] - \left[\frac{\partial L(q,\, \dot{q})}{\partial q}\right] + f_f(f_e,\, \dot{q}), \quad (1)$$

Table 2. PSO parameters.

Parameter	Value
Cognitive factor (c_1)	1.2
Social factor (c_2)	0.12
Inertia weight (w)	0.9
No. of particles (n)	30
Max iteration	30
Dimension (dim)	3
Random values ($r_1,\ r_2$)	rand(dim, n)
Initial conditions ($K_p,\ K_i,\ K_d$)	25, 5, 5

Table 3. Objective function values considering heuristic method.

Parameter	Value
Hip	11.13
Knee	15.33
Ankle	9.936

where, $\tau = [\tau_1 \quad \tau_2 \quad \tau_3]^T$ is the joint pairs vector, $q = [q_1 \quad q_2 \quad q_3]^T$ is the angular positions vector, $\dot{q} = [\dot{q_1} \quad \dot{q_2} \quad \dot{q_3}]^T$ is the angular velocities vector, $L(q,\ \dot{q})$ is the Lagrangian function and $f_f(f_e,\ \dot{q})$ is a friction function. The Lagrangian function is given by the following:

$$L(q,\ \dot{q}) = K_i(q,\ \dot{q}) - U_i(q), \quad i = 1, 2, 3, \tag{2}$$

where, $K_i(q,\ \dot{q})$ is the kinetic energy and $U_i(q)$ is the potential energy. The kinetic energy of each bond of a mechanism is defined as:

$$K_i(q, \dot{q}) = \frac{1}{2}\left[m_i\ v_i^T\ v_i + I_i\ \dot{q}^2\right], \tag{3}$$

where, m_i is the mass of the link to be analyzed, v_i is the linear speed of the link and I_i is the moment of inertia tensor of the link. On the other hand, potential energy is defined as:

$$U_i(q) = m_i\ g\ h_i, \tag{4}$$

where, g is the ground gravity constant and h_i is the current height of the link with respect to the ground. To construct the equation of motion the equations (3) and (4) are replaced in the equation (2), the corresponding derivatives are calculated and thus the equation (1) is obtained.

Friction terms are not considered for this problem. A common way to represent the result of evaluating equation (1) is the so-called dynamic model in matrix form defined as [17]:

$$\tau = M(q)\ddot{q} + C(q, \dot{q})\ \dot{q} + G(q), \tag{5}$$

where, $\ddot{q} = [\ddot{q_1} \quad \ddot{q_2} \quad \ddot{q_3}]^T$ refers to the vector of angular accelerations, $M(q)$ is the inertial matrix, $C(q,\ \dot{q})$ is the matrix of centripetal forces and the gravity pair vector,

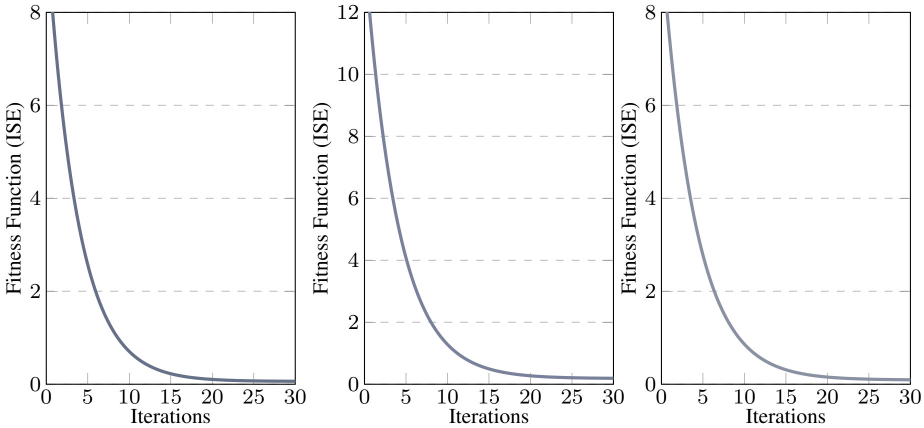

(a) (b) (c)

Fig. 3. (a) Fitness objective function for the hip trajectory, (b) fitness objective function for the knee trajectory (c) fitness objective function for the ankle trajectory.

denoted as $G(q)$:

$$M(q) = \begin{bmatrix} M_{11} & M_{12} & M_{13} \\ M_{21} & M_{22} & M_{23} \\ M_{31} & M_{32} & M_{33} \end{bmatrix}, \tag{6}$$

where:

$$\begin{aligned}
M_{11} &= I_1 + I_2 + I_3 + \ell_1^2\, m_2 + \ell_1^2\, m_3 + \ell_2^2\, m_3 + \ell_{c_1}^2\, m_1 + \ell_{c_2}^2\, m_2 + \ell_{c_3}^2\, m_3 + 2\, \ell_1\, \ell_{c_3}\, m_3 \\
&\quad \operatorname{Cos}(q_2 + q_3) + 2\, \ell_1\, \ell_2\, m_3 \operatorname{Cos}(q_2) + 2\, \ell_1\, \ell_{c_2}\, m_2 \operatorname{Cos}(q_2) + 2\, \ell_2\, \ell_{c_3}\, m_3 \operatorname{Cos}(q_3), \\
M_{12} &= I_2 + I_3 + m_3\Big(\ell_2^2 + 2\, \ell_2\, \ell_{c_3} \operatorname{Cos}(q_3) + \ell_1\, \ell_2 \operatorname{Cos}(q_2) + \ell_{c_3}^2 + \ell_1\, \ell_{c_3} \operatorname{Cos}(q_2 + q_3)\Big) + \\
&\quad \ell_{c_2}\, m_2\Big(\ell_{c_2} + \ell_1 \operatorname{Cos}(q_2)\Big), \\
M_{13} &= I_3 + \ell_{c_3}\, m_3\Big(\ell_{c_3} + \ell_1 \operatorname{Cos}(q_2 + q_3) + \ell_2 \operatorname{Cos}(q_3)\Big), \\
M_{21} &= I_2 + I_3 + m_3\Big(\ell_2^2 + 2\, \ell_2\, \ell_{c_3} \operatorname{Cos}(q_3) + \ell_1\, \ell_2 \operatorname{Cos}(q_2) + \ell_{c_3}^2 + \ell_1\, \ell_{c_3} \operatorname{Cos}(q_2 + q_3)\Big) + \\
&\quad \ell_{c_2}\, m_2\Big(\ell_{c_2} + \ell_1 \operatorname{Cos}(q_2)\Big), \\
M_{22} &= I_2 + I_3 + \ell_{c_2}^2\, m_2 + m_3\Big(\ell_2^2 + 2\, \ell_2\, \ell_{c_3} \operatorname{Cos}(q_3) + \ell_{c_3}^2\Big), \\
M_{23} &= I_3 + m_3\Big(\ell_{c_3}^2 + \ell_2\, \ell_{c_3} \operatorname{Cos}(q_3)\Big), \\
M_{31} &= I_3 + \ell_{c_3}\, m_3\Big(\ell_{c_3} + \ell_1 \operatorname{Cos}(q_2 + q_3) + \ell_2 \operatorname{Cos}(q_3)\Big), \\
M_{32} &= I_3 + m_3\Big(\ell_{c_3}^2 + \ell_2\, \ell_{c_3} \operatorname{Cos}(q_3)\Big), \\
M_{33} &= I_3 + \ell_{c_3}^2\, m_3.
\end{aligned}$$

$$C(q,\dot{q}) = \begin{bmatrix} C_{11} & C_{12} & C_{13} \\ C_{21} & C_{22} & C_{23} \\ C_{31} & C_{32} & C_{33} \end{bmatrix}, \tag{7}$$

where:

$$\begin{aligned}
C_{11} =& \quad 0,\\
C_{12} =& -2\,\ell_1\,\dot{q_1}\Big(\ell_2\,m_3\,\mathrm{Sen}(q_2) + \ell_{c_2}\,m_2\,\mathrm{Sen}(q_2) + \ell_{c_3}\,m_3\,\mathrm{Sen}(q_2+q_3)\Big) - \ell_1\,\dot{q_2}\Big(\ell_2\,m_3\\
&\mathrm{Sen}(q_2) + \ \ell_{c_2}\,m_2\,\mathrm{Sen}(q_2) + \ell_{c_3}\,m_3\,\mathrm{Sen}(q_2+q_3)\Big) - \ell_1\,\ell_{c_3}\,m_3\,\dot{q_3}\,\mathrm{Sen}(q_2+q_3),\\
C_{13} =& -\ \dot{q_1}\Big(2\,\ell_1\,\ell_{c_3}\,m_3\,\mathrm{Sen}(q_2+q_3) + 2\,\ell_2\,\ell_{c_3}\,m_3\,\mathrm{Sen}(q_3)\Big) - m_3\,\dot{q_2}\Big(2\,\ell_2\,\ell_{c_3}\,\mathrm{Sen}(q_3)\\
&+\ \ell_1\,\ell_{c_3}\,\mathrm{Sen}(q_2+q_3)\Big) - \ell_{c_3}\,m_3\,\dot{q_3}\Big(\ell_1\,\mathrm{Sen}(q_2+q_3) + \ell_2\,\mathrm{Sen}(q_3)\Big),\\
C_{21} =& \quad 0,\\
C_{22} =& -\dot{q_1}\Bigg(m_3\Big(\ell_1\,\ell_2\,\mathrm{Sen}(q_2) + \ell_1\,\ell_{c_3}\,\mathrm{Sen}(q_2+q_3)\Big) + \ell_1\,\ell_{c_2}\,m_2\,\mathrm{Sen}(q_2)\Bigg),\\
C_{23} =& -\ell_{c_3}\,m_3\Big(2\,\ell_2\,\dot{q_1}\,\mathrm{Sen}(q_3) + 2\,\ell_2\,\dot{q_2}\,\mathrm{Sen}(q_3) + \ell_2\,\dot{q_3}\ \mathrm{Sen}(q_3) + \ell_1\,\dot{q_1}\,\mathrm{Sen}(q_2+q_3)\Big),\\
C_{31} =& \quad 0,\\
C_{32} =& -\ell_1\,\ell_{c_3}\,m_3\,\dot{q_1}\,\mathrm{Sen}(q_2+q_3),\\
C_{33} =& -\ell_{c_3}\,m_3\,\dot{q_1}\Big(\ell_1\,\mathrm{Sen}(q_2+q_3) + \ell_2\,\mathrm{Sen}(q_3)\Big) - \ell_2\,\ell_{c_3}\,m_3\,\dot{q_2}\,\mathrm{Sen}(q_3).
\end{aligned}$$

$$G(q) = \begin{bmatrix} G_1 \\ G_2 \\ G_3 \end{bmatrix}, \tag{8}$$

where:

$$\begin{aligned}
G_1 &= g\,m_3\Big(\ell_2\,\mathrm{Sen}(q_1+q_2) + \ell_1\,\mathrm{Sen}(q_1) + \ell_{c_3}\,\mathrm{Sen}(q_1+q_2+q_3)\Big) +\\
&\quad g\,m_2\Big(\ell_{c_2}\,\mathrm{Sen}(q_1+q_2) + \ell_1\,\mathrm{Sen}(q_1)\Big) + 2\,g\,\ell_{c_1}\,m_1\,\mathrm{Sen}(q_1),\\
G_2 &= g\,m_3\Big(\ell_2\,\mathrm{Sen}(q_1+q_2) + \ell_{c_3}\,\mathrm{Sen}(q_1+q_2+q_3)\Big) + g\,\ell_{c_2}\,m_2\,\mathrm{Sen}(q_1+q_2),\\
G_3 &= g\,\ell_{c_3}\,m_3\,\mathrm{Sen}(q_1+q_2+q_3).
\end{aligned}$$

3 Exoskeleton Control System

Dynamic models can be examined through the approach of both linear and nonlinear systems. In the context of control system tuning, a heuristic approach is often employed for linear systems, while intelligent algorithms are typically harnessed when dealing with nonlinear systems. The heuristic tuning method in control is based on empirically adjusting the parameters of a controller rather than using a purely analytical or theoretical approach.

Table 4. Objective function values considering intelligent method.

Parameter	Value
Hip	0.1074
Knee	0.2328
Ankle	0.1341

This approach is used when the system is complex and optimal controller parameter values cannot be calculated directly. Intelligent tuning methods for control are based on the use of artificial intelligence (AI) or machine learning (ML) techniques to automatically adjust and optimize the parameters of a control system [25]. To illustrate the operation of the proposed design in the reproduction of lower limb movements, it is proposed to solve a trajectory tracking control problem using a PID control scheme that calculates the torque for each of the exoskeleton joints.

3.1 Control Scheme

It is considered $q_d = [q_{d_1} \;\; q_{d_2} \;\; q_{d_3}]^T$ as the reference trajectories to be reproduced on each of the legs of the exoskeleton, then considering the angular position $q = [q_1 \;\; q_2 \;\; q_3]^T$, the position error is defined as the vector:

$$e(t) = \begin{bmatrix} q_{d_1}(t) - q_1(t) \\ q_{d_2}(t) - q_2(t) \\ q_{d_3}(t) - q_3(t) \end{bmatrix}, \tag{9}$$

From the error vector $e(t)$, the PID law control [16] is defined as:

$$\tau = K_p \, e(t) + K_v \, \dot{e}(t) + K_i \int_0^t e(t) \, dt, \tag{10}$$

where $\tau = [\tau_1 \;\; \tau_2 \;\; \tau_3]^T$ are the pairs in the three joints of each leg and K_p, K_v y $K_i \in R^{3\times3}$ are the defined positive gain matrices, called proportional, derivative and integral gain, respectively. To solve the control problem, the reference trajectories q_d are then required. In this work, the data reported in [18] about the angular positions of the hip, knee, and ankle (both legs) in study subjects who performed walking activities were used as reference trajectories.

3.2 Optimization of the Controller´s Gains

The numeric value of the gain matrices is calculated based on Particle Swarm Optimization algorithm (PSO), such that the closed-loop system response converges to the proposed input reference. PSO is an optimization technique inspired by the cooperative patterns observed in nature, such as the flocking of birds and the schooling of fish.

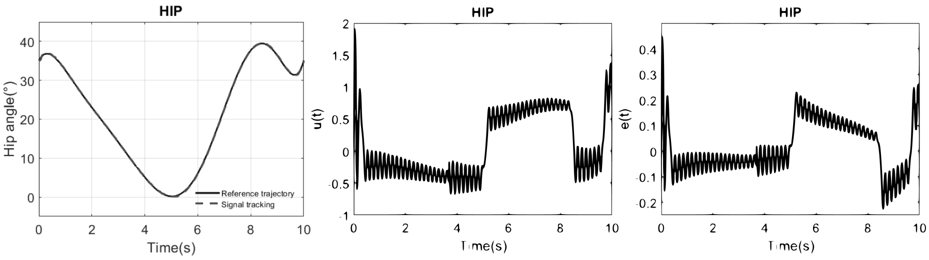

(a) (b) (c)

Fig. 4. (a) Trajectory tracking signal, (b) input torque and (c) trajectory error signal, of the hip joint.

Table 5. Calculated gains from PSO algorithm.

Joint	K_p	K_i	K_d
Hip	240.9220	122.7799	23.8527
Knee	210.6642	131.6928	3.45810
Ankle	241.7013	27.69170	17.6263

It is a metaheuristic approach that exhibits several advantages: PSO necessitates minimal or no assumptions regarding the optimization problem at hand, it does not depend on problem differentiability, and it can explore vast solution spaces. These attributes make PSO a potent tool for tackling multidimensional and intricate optimization problems.

Within the framework of the PSO algorithm, the particles, representing potential solutions, navigate through the search space by aligning their movements with the current optimal particle. Essentially, at the k-th iteration, each particle p_i in the swarm possesses two attributes: its position denoted as $X(t)$ and its velocity denoted as $V(t)$.

The particle's motion is determined in terms of velocity that combines the influence of its own best position P_{best} and the collective best position of the complete swarm G_{best} inside the exploration domain:

$$V(t+1) = w\, V(t) + c_1\, r_1\, \left(P_{\text{best}} - X(t)\right) + c_2\, r_2 \left(G_{\text{best}} - X(t)\right), \tag{11}$$

$$X(t+1) = X(t) + V(t+1). \tag{12}$$

More precisely, the speed of each individual particle undergoes an update using Equation (11). In this equation, the cognitive and social learning coefficients are represented by c_1 and c_2, respectively. The prescribed inertia weight is represented by w, while r_1 and r_2 denote random numbers generated within the range of 0 and 1 during each iteration. The particle's position can be updated using Equation (12). The iteration process concludes either when the predetermined number of iterations is attained or when the objective function $f(t)$ reaches a critical value [11].

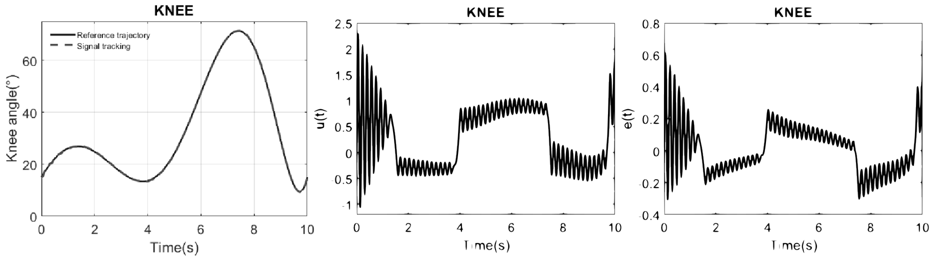

(a) (b) (c)

Fig. 5. (a) Trajectory tracking signal, (b) input torque and (c) trajectory error signal, of the knee joint.

3.3 Objective Functions

Selecting the objective functions to assess the fitness of each particle stands as a pivotal step in the implementation of PSO [15]. Among the objective functions commonly employed are the Mean Squared Error (MSE), the Integral of Time multiplied by Absolute Error (ITAE), the Integral of Absolute Error (IAE), and the Integral of Squared Error (ISE) [7]. In this study, the objective function employed is ISE due to its minimal energy consumption in the context of energy control [13] and is described by the following equation:

$$\text{ISE} = \int_0^t e^2(t)\, dt, \tag{13}$$

where $e(t)$ is the error signal and is based in Equation (9).

4 Experiment Design

The simulation of the exoskeleton experiment as shown in Figure 2, is developed in Matlab-Simulink considering a mathematical model of 1 DOF, the trajectory input signals, the PID control system and the PSO intelligent tuning method using ISE as objective function. The decision variables considered in the PSO algorithm are based on the minimization of the objective function ISE, when PSO finds a better population of particles, the value of the objective function is updated until the end of the simulation by restricting the iterations.

It is well known that the PID control law does not generate an equilibrium point of the closed-loop system with global asymptotic stability characteristics, it only has local asymptotic stability as long as the gains are positive defined, therefore, the algorithm has the constraint of only looking for positive gain values such that the closed-loop system response converges to the reference trajectories.

It is important to mention that ISE function global minimum value is 0. Thus, PSO algorithm works to optimize the objective function to zero that is equals to calculate a minimum trajectory tracking error.

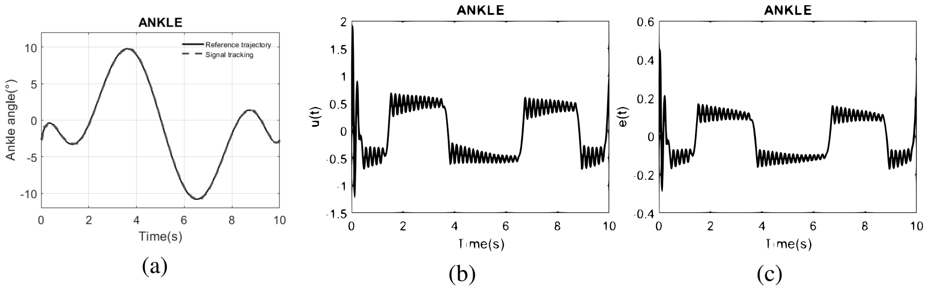

Fig. 6. (a) Trajectory tracking signal, (b) input torque and (c) trajectory error signal, of the ankle joint.

Then, the optimization problem can be defined as follows:

$$e(t) = q_{di}(t) - q_i(t), \text{ such that, } \mathrm{ISE} = \int_0^t e^2(t)\, dt = 0 \quad \text{(Global minimum)}, \quad (14)$$

considering that, K_p, K_i and $K_d \in R^+$. Thus:

$$\tau = K_p\, e(t) + K_v\, \dot{e}(t) + K_i \int_0^t e(t)\, dt, \text{ converge to trajectory signals.} \quad (15)$$

As mentioned in subsection 3.1, the trajectory input signals was taken from [18] and the acceleration of the 1 DOF dynamical model is calculated as follow:

$$\ddot{q} = \frac{\left[\tau - m\, g\, \ell_c \,\mathrm{Sen}\, q - b\, \dot{q} - f_c\ \mathrm{signo}(\dot{q})\right]}{\left[\ell_c^2 + I\right]}. \quad (16)$$

The parameters used to simulate the dynamic model are shown in Table 1. The experiment parameters to simulate the PSO are presented in Table 2 and as mentioned in subsection 3.3, ISE is used as objective function based on the error signal from the closed-loop system. Table 3 shows the objective function calculated values based on the heuristic method. Also, gain values from heuristic method were used as initial conditions for the intelligent method. Objective function for the three joints during the iterative process of the intelligent method is presented in Figure 3 and the calculated values are presented in Table 4.

5 Results

Having considered the previous work, this section presents the results of the dynamic model from the Euler Lagrange motion equations and the solution of the trajectory tracking control problem using a PID schema based in PSO to find the best gain values based on ISE objective function. The calculated gain values are presented in Table 5. The results of tracking, input torque and error for joints are shown in Figures 4, 5 and 6.

6 Conclusions

Utilizing conventional methods to implement a controller for a multiple joint structure proves to be challenging and lacks precision. Integrating intelligent swarm optimization techniques, such as PSO, presents a viable approach for fine-tuning PID controllers. As mentioned in subsection 3.3, there is a range of objective functions available for consideration.

However, within the context of energy control, ISE was selected as the objective function to be optimized by the PSO algorithm for tuning the PID controller gains. Results shows that the tuned controller scheme generate adequate torques to accomplish the trajectory tracking problem. The intelligent method calculates better performance values in terms of angular position error, so considering the generated gains, the low-level control was improved compared with the heuristic method.

References

1. Baud, R., Manzoori, A. R., Ijspeert, A., Bouri, M.: Review of control strategies for lower-limb exoskeletons to assist gait. Journal of NeuroEngineering and Rehabilitation, vol. 18, no. 1 (2021) doi: 10.1186/s12984-021-00906-3
2. Biao, L., Youwei, L., Xiaoming, X., Haoyi, W., Longhan, X.: Design and control of a flexible exoskeleton to generate a natural full gait for lower-limb rehabilitation. Journal of Mechanisms and Robotics, vol. 15, no. 1 (2022) doi: 10.1115/1.4054248
3. Brault, M.: Americans with disabilities: Current population reports (2010) www.census.gov/library/publications/2012/demo/p70-131.html
4. CDC: Division of birth defects and developmental disabilities, data and statistics (2020) www.cdc.gov
5. Chan, M., Zoellick, R. B.: World report on disability (2011) iris.who.int/bitstream/handle/10665/44575/9789240685215_eng.pdf?sequence=1
6. Eurostat: Population by type of basic activity difficulty, sex and age (2019) ec.europa.eu/eurostat/databrowser/view/HLTH_DP040/default/table?lang=en&category=hlth.hlth_dsb.hlth_dsb_prv
7. Griffin, I., Bruton, J.: On-line PID controller tuning using genetic algorithms Dublin City University (2003)
8. Gutiérrez, J. P., Rivera-Dommarco, J., Shamah-Levy, T., Villalpando-Hernández, S., Franco, A., Cuevas-Nasu, L., Romero-Martínez, M., Hernández-Ávila, M.: Encuesta nacional de salud y nutrición. Resultados nacionales (2012) ensanut.insp.mx/encuestas/ensanut2012/doctos/informes/ENSANUT2012ResultadosNacionales.pdf
9. Kelly, R.: Control de movimiento de robots manipuladores. Pearson Education (2003)
10. Kim, H., June-Shin, Y., Kim, J.: Design and locomotion control of a hydraulic lower extremity exoskeleton for mobility augmentation. Mechatronics, vol. 46, pp. 32–45 (2017) doi: 10.1016/j.mechatronics.2017.06.009
11. Liu, J., Fang, H., Xu, J.: Online adaptive PID control for a multi-joint lower extremity exoskeleton system using improved particle swarm optimization. Machines, vol. 10, no. 1, pp. 21 (2021) doi: 10.3390/machines10010021
12. Mackay, J., Mensah, G.: World health organization: The atlas of heart disease and stroke (2004) apps.who.int/iris/handle/10665/43007

13. Maghfiroh, H., Saputro, J. S., Hermanu, C., Ibrahim, M. H., Sujono, A.: Performance evaluation of different objective function in PID tuned by PSO in DC-motor speed control. In: Proceedings of the IOP Conference Series: Materials Science and Engineering, vol. 1096 (2021) doi: 10.1088/1757-899x/1096/1/012061
14. Mayo Clinic: Accidente cerebrovascular (2022) www.mayoclinic.org
15. Mirzal, A., Yoshii, S., Furukawa, M.: PID parameters optimization by using genetic algorithm. Journal of International Science and Technology Conference, vol. 8, pp. 34–43 (2006) doi: 10.48550/arXiv.1204.0885
16. Ogata, K.: Ingeniería de control moderna. Pearson Education (2010)
17. Reyes, F.: Robótica: control de robots manipuladores. Alfa Omega (2011)
18. Ribeiro, T. S., de-Sousa, A. C., de-Lucena, L. C., Santiago, L. M. M., Lindquist, A. R. R.: Does dual task walking affect gait symmetry in individuals with Parkinson's disease? European Journal of Physiotherapy, vol. 21, no. 1, pp. 8–14 (2018) doi: 10.1080/21679169.2018.1444086
19. Sharifi, M., Mehr, J. K., Mushahwar, V. K., Tavakoli, M.: Adaptive CPG-based gait planning with learning-based torque estimation and control for exoskeletons. IEEE Robotics and Automation Letters, vol. 6, no. 4, pp. 8261–8268 (2021) doi: 10.1109/lra.2021.3105996
20. Soleimani-Amiri, M., Ramli, R., Ibrahim, M. F., Abd-Wahab, D., Aliman, N.: Adaptive particle swarm optimization of pid gain tuning for lower-limb human exoskeleton in virtual environment. Mathematics, vol. 8, no. 11 (2020) doi: 10.3390/math8112040
21. Tibaduiza-Burgos, D. A., Aya-Parra, P. A., Anaya-Vejar, M.: Exoesqueleto para rehabilitación de miembro inferior con dos grados de libertad orientado a pacientes con accidentes cerebrovasculares. INGE CUC, vol. 15, no. 2, pp. 36–47 (2019) doi: 10.17981/ingecuc.15.2.2019.04
22. Tovar-Estrada, M., Rodriguez-Liñan, A., Quiroz, G.: Implementation of a scale-lab lower-limb exoskeleton with motion in three anatomical planes. Cybernetics and Systems, vol. 50, no. 6, pp. 516–538 (2019) doi: 10.1080/01969722.2019.1630565
23. World Health Organization: Spinal cord injury (2013) www.who.int/news-room/fact-sheets/detail/spinal-cord-injury
24. World Health Organization: Congenital anomalies (2022) www.who.int/health-topics/congenital-anomalies#tab=tab_1
25. Yu, W.: PID Control with Intelligent Compensation for Exoskeleton Robots. Elsevier (2018) doi: 10.1016/C2016-0-04547-3